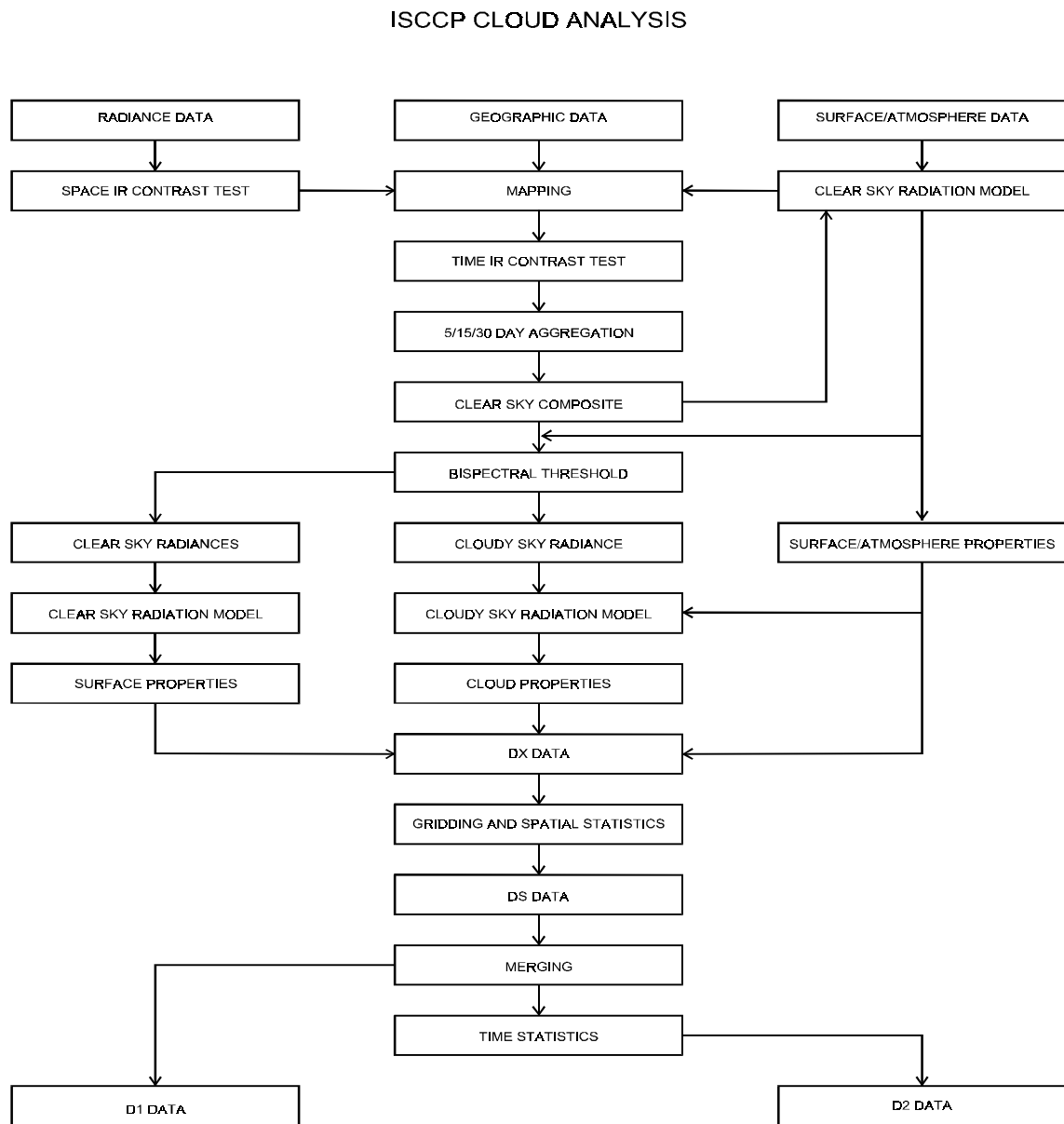


## 3.2. PIXEL LEVEL ANALYSIS (STAGE DX)

### 3.2.1. OVERVIEW

The ISCCP cloud analysis, shown schematically in Figure 3.4, is applied separately to the Stage B3 radiance data (Schiffer and Rossow 1985; Rossow et al. 1987) from each satellite, together with the TV and IS datasets (see Sections 6.1 and 6.2). The absolute radiometric calibrations of all Stage B3 radiances have been normalized to that of the NOAA-9 AVHRR (Brest and Rossow 1992, Brest et al. 1996; Desormeaux et al. 1993; Rossow et al. 1992, 1996). The analysis is composed of two



**Figure 3.4.** Schematic of ISCCP cloud analysis.

major procedures: the cloud detection procedure divides the B3 radiances into cloudy and clear groups and the radiative analysis procedure retrieves physical properties of clouds and the surface, respectively.

The cloud detection procedure (Section 3.2.4) analyzes the radiance data in four steps: the first two steps represent the original cloud detection procedure used to produce the C-series of cloud products (Rossow and Garder 1993a) with minor revisions and the second two steps are refinements added to produce the D-series cloud products. The first step uses a series of tests of the space-time variations of the IR and VIS radiances to obtain the first estimate of the radiance values that represent clear conditions at each place and time. The second determines which radiance measurements deviate from the first clear sky values by an amount greater than the uncertainty in the estimated clear radiances (first threshold test). The third step conducts an additional series of tests, based on the results of the first two steps, to remove some infrequent errors in the clear sky radiances that occur under certain circumstances. For polar orbiter data, the third step also obtains an estimate of the daytime clear solar reflectances for the near-infrared channel. Together these results are the refined clear-sky radiances. The fourth step is the final threshold test using the refined clear sky radiances and, in the case of polar orbiter data, an additional threshold test for near-infrared radiances over ice and snow-covered surfaces. Cloudy conditions are **defined** by those radiances that are sufficiently different from the clear values in any spectral channel.

The radiation analysis procedure (Section 3.2.5) first retrieves the properties of the surface from the clear sky composite radiances and the atmospheric data for each pixel (ranging from 4 to 7 km in size). These surface properties are then used, along with the same atmospheric properties, to analyze individual pixel radiances. For each individual pixel, **either** surface properties or cloud properties are retrieved from the pixel radiances depending on whether the threshold tests indicate clear or cloudy conditions. When only IR data are available, all clouds are assumed to be completely opaque to IR radiation. When both VIS and IR data are available (daytime only), the IR retrieval is adjusted to account for the effects of variable cloud optical thickness on the radiances. Both the unadjusted (IR only) and VIS-adjusted results are reported in daytime. For the C-series cloud products, the VIS/IR analysis used a single microphysical model representing a liquid water cloud to analyze all clouds. In the D-series cloud products, the analysis uses two models: the original liquid water cloud model and an ice crystal microphysical model. In daytime conditions in the polar regions over snow or sea ice, NIR reflectances are used to aid in the retrieval of cloud optical thicknesses.

### 3.2.2. MAP PROJECTIONS

The input radiance dataset (Stage B3) is in "image" form, a projection of the Earth onto the image plane at the satellite detector; however, motions of the satellites cause variations of the relation between image position and geographic location. To compare the radiances at the same location over the whole month, as required in the cloud detection procedure, all satellite images for each satellite and month are re-mapped into fixed map projections so that each array position represents a fixed latitude/longitude. For the geostationary satellites, the map projections approximate the original image with the sub-satellite latitude/longitude fixed for the whole month (Figure 3.5); these positions may vary from month to month. The GOES and GMS data use the General Perspective, spherical equations (U.S. Geological Survey Bulletin 1532); METEOSAT and INSAT data are projected into fixed views by the satellite operators that appear similar to the General Perspective projections. For the polar orbiter data, two different map projections are used: a simple latitude/longitude grid at low latitudes (between  $-50^\circ$  and  $50^\circ$ ) and a Lambert Azimuthal Equal-Area projection (U.S. Geological Survey Bulletin 1532) for the two polar regions (Figure 3.6).

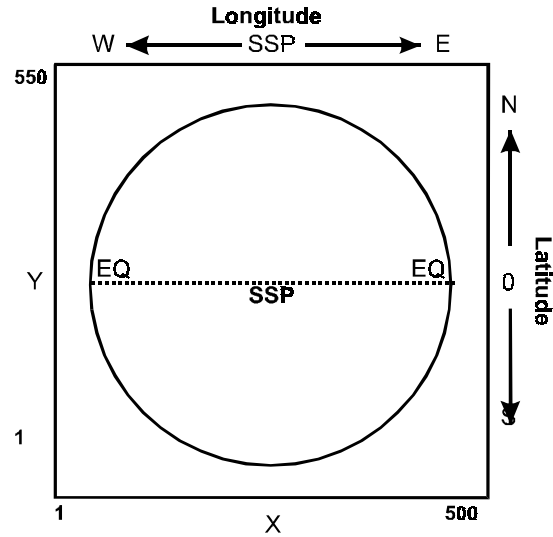


**Figure 3.5.** Geostationary projection with nominal sub-satellite point (SSP) on the equator at a specified longitude. The X,Y coordinates indicate position within DX data array.

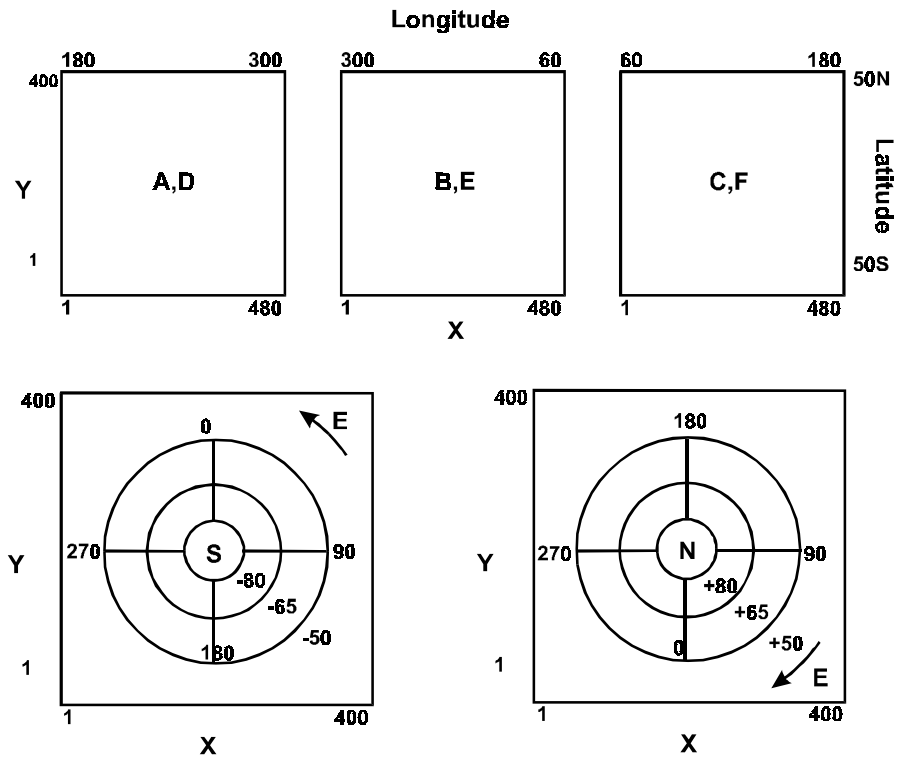


**Figure 3.6.** Geographic regions for polar orbiter DX data. Lower latitudes (A-F) in latitude-longitude grids and two polar cap projections (S, N). The X,Y coordinates indicate position within DX data array.

The original radiance data represent measurements over fields-of-view (FOV) ranging from 4 to 7 km in size at nadir (pixels); however, the Stage B3 data are sampled to a spacing of about 25-30 km. Although navigation accuracy may be higher for some satellites, overall accuracy is confirmed to be about  $\pm 25$  km. The analysis to determine clear radiances uses the sampled data mapped to 25 km resolution; hence, we consider the smaller individual image pixels to represent a *sample* of the distribution of surface and cloud conditions over this larger spatial scale. Although the variability of surfaces and clouds is generally smaller at such small scales than at scales  $\sim 100$  km (Sèze and Rossow 1991), all pixel-level quantities are treated as having a certain amount of intrinsic variation about an average value representing the spatial domain of approximately 25 km in size. In any case, the cloud detection tests and radiative analysis are applied to the original image pixels, so we will continue to refer to the smallest unit of data as a pixel, whether it is the original image pixel or the small 25 km domains from the mapped images.

### 3.2.3. VARIABLE DEFINITIONS

#### Land/Water

At pixel level the basic surface type is either land or water; pixels labeled as coast in the Stage B3 dataset are discarded.

#### Day/Night

Pixels with  $MU0 < 0.2$  (solar zenith angle  $> 78.5$  degrees) are labeled "night". If  $MU0 \geq 0.2$  and VIS information is available, the pixel is labeled "day". If any VIS radiance information is missing and  $MU0 < 0.3$ , the pixel status is changed to "night", otherwise it is discarded.

To avoid spurious diurnal variations of cloudiness caused by changes in methodology associated with the presence or absence of VIS data, the results of two separate analyses are reported during the daytime: one dependent on both VIS and IR information (including NIR results) and one dependent only on IR information. Clear sky IR and VIS radiances are determined independently and all threshold decisions are recorded separately. (Clear sky NIR radiances are also determined independently.)

#### Viewing Geometry

Satellite viewing geometry is defined by the cosine of the satellite zenith angle at the surface point ( $MUE = 0 - 1$ ); the solar illumination geometry is defined by the cosine of the solar zenith angle at the surface point ( $MU0 = 0 - 1$ ) and the relative azimuth angle between the solar and satellite vectors to the surface point ( $PHI = 0^\circ - 180^\circ$ ). *Note: In radiative transfer applications, the relative azimuth angle that is reported is defined as  $180^\circ$  minus the usual geometric relative azimuth angle, which is the difference of two position azimuth angles.*

#### Radiances

Infrared (wavelength  $> 3 \mu\text{m}$ ) radiances are reported as brightness temperatures in Kelvins (165 K - 345 K). Shortwave (wavelength  $< 3 \mu\text{m}$ ) radiances are expressed as scaled radiances, fractions from zero to 1.108. Scaled radiances are calculated by dividing the measured radiance by the value that would be

reflected from a surface with albedo = 1 at the mean sun-Earth distance weighted by the instrument response function.

### Cloudy/Clear Decision (Threshold Results)

For each pixel in the DX dataset, the results of all threshold tests are recorded by reporting the relative relationship between the pixel radiances and the corresponding clear sky radiances. The numerical codes for each radiance indicate how far the particular pixel radiance is from the clear sky value in intervals of the threshold magnitude (see Table 2.5.5 and Figure 3.2).

A pixel is considered cloudy if **any** of the following threshold results is reported: IR code = 4, 5; VIS code = 4, 5 or NIR code = 9, 10, 11, 12 and 13. A clear pixel occurs only when all threshold results indicate clear.

### Cloud Retrievals

Cloud top temperature/pressure values are obtained using three different radiative models: blackbody, liquid water droplet cloud ( $r_e = 10 \mu\text{m}$ ) and ice polycrystal cloud ( $r_e = 30 \mu\text{m}$ ). The first retrieval model assumes that all clouds are blackbodies, i.e., the cloud emission temperature, corrected for atmospheric water vapor effects, is its physical temperature. This assumption is equivalent to assuming that all clouds are opaque ( $\text{TAU} > 10$ ) and non-scattering and the results are independent of cloud optical thickness. These values (ITMP and IPRS) are reported for all clouds at all times of day. The other two models determine cloud top temperatures and pressures by correcting for variations in cloud emission and scattering that are functions of the optical thickness and particle size/shape. The results obtained assuming a liquid water cloud model are reported for all cloudy pixels as  $\text{TAU} = \text{VALBTA}$ ,  $\text{TC} = \text{VTMP}$  and  $\text{PC} = \text{VPRS}$ . The results obtained assuming a ice crystal cloud model are reported as  $\text{TAU} = \text{VTAUIC}$ ,  $\text{TC} = \text{VTMPIC}$  and  $\text{PC} = \text{VPRSIC}$  when  $\text{VTMPIC} < 273 \text{ K}$ .

### Clear Retrievals

Surface "skin" temperatures (TS) in Kelvins are obtained from clear IR radiances by assuming that the surface emission temperature, corrected for atmospheric water vapor effects, is its physical temperature. This assumption is equivalent to assuming a surface emissivity of unity at  $\approx 11 \mu\text{m}$  wavelength. Values of TS retrieved from the clear sky composite radiances are present for all pixels (ICSTMP). If the pixel is clear, then ITMP represents the surface temperature retrieved from the measured radiance. The corresponding surface pressures are ICSPRS for the clear sky composite analysis and IPRS for a clear pixel.

Visible ( $\approx 0.6 \mu\text{m}$  wavelength) reflectances (RS), reported as fractions from 0 to 1.108, are obtained from clear VIS radiances of daytime pixels by correcting for variable sun-Earth distance and for Rayleigh scattering and ozone absorption in the atmosphere. The surface is assumed to be an isotropic scatterer in the retrieval, which introduces only a small error for darker surfaces; the actual viewing/illumination geometry is given for each pixel. Values of RS retrieved from the clear sky composite radiances are present for all daytime pixels ( $\text{RS} = \text{VCSALB}$ ). If the pixel is clear, then VALBTA represents the surface visible reflectance retrieved from the measured radiance.

### 3.2.4. CLOUD DETECTION

The first version of the cloud detection procedure is described by Rossow and Garder (1993a, 1993b, see also Rossow *et al.* 1991). Validation is described in Rossow and Garder (1993b) and Rossow *et al.* (1993). The new cloud detection procedure is composed of the original steps, with four minor modifications, plus two new steps.

#### 3.2.4.1. FIRST CLEAR SKY RADIANCES

Clear radiance values are needed for every location at each time (each day for each 3 hour period, separately). Since clouds obscure the view of the surface at some times and do so more or less frequently in different climate regimes, the object of the analysis is to infer the unseen values from the observed values. The accuracy of this procedure is dependent on the frequency of cloudiness at each location (see Rossow *et al.* 1989 and Rossow and Garder 1993a for reviews of the history of methods to detect clouds).

In the first cloud detection step, four basic premises are used to identify clear pixels from an examination of the spatial and temporal variations of radiances: (1) clear pixels are assumed to exhibit less spatial and/or temporal variability than cloudy pixels, (2) clear pixels are assumed to be warmer (larger IR radiance) and/or darker (lower VIS radiance) than cloudy pixels, (3) the first two characteristics vary with surface type (climate regime), and (4) no single test is reliable under all conditions for all cloud types. If the time comparisons are arranged in daily sequences for each UTC separately to avoid confusion with the generally larger diurnal variations of the surface and of the solar illumination, then the time variability tests are much more reliable indicators of cloudiness than the space variability tests. The clear sky radiances are estimated at all locations and times from the result of two tests and the accumulation of three kinds of statistics over two spatial domains and three time periods. The test parameters vary with location to give preference to one type of test over another depending on local characteristics. All these tests are conservative in that any "hint" of contamination is used to discard values, including some actually clear values, to ensure the accuracy of the resulting clear sky radiance values.

The clear sky analysis procedure provides an **estimate** of the clear radiances for every 25 km scene (now called pixel) every three hours; however, the effective space/time resolution attained is about 75 km (IR) or 25 km (VIS and NIR) and 5-days (IR) or 30-days (VIS and NIR). If cloudiness is very frequent, the effective time resolution for IR clear radiances may be reduced to 15 or 30 days. Diurnal variations are resolved, however, by conducting the whole analysis separately at eight diurnal phases.

#### Surface Types and Correlative Data

Four correlative data sets are used to specify different surface types as a function of latitude/longitude: (1) land/water/coast classification (based on a revision of Masaki 1972), (2) topographic height (U.S. Navy dataset from NCAR), (3) land vegetation type (based on Matthews 1983), and (4) sea ice/snow cover (Section 6.2). Individual pixels identified as coast are roughly equal mixtures of land and water at a scale of 25 km and are discarded. The IR clear sky logic uses four different surface types, in order of increasing variability, and the VIS clear sky logic uses eleven surface types (Table 3.2.1).

**Table 3.2.1. Surface Types Used in Clear Sky Analysis.**

| TYPE    | DEFINITION  |
|---------|---|
| IR 1    | "low variability" water - all open water except Type 2  |
| IR 2    | "high variability" water - water within 75 km of a coastline, water within 50 km of sea ice, or sea ice-covered water   |
| IR3     | "low variability" land - all open land (including land within 50 km of a coastline) or snow-covered land except Type 4  |
| IR4     | "high variability" land - high topography pixels (height > 1750 m), all pixels within 300 km regions that are rough topography (standard deviation of heights > 1000 m) or that are high topography (mean height > 2500 m), or permanently ice-covered locations (Iceland, Greenland and Antarctica). |
| VIS 1   | all open water including near-coastal   |
| VIS 2   | sea ice-covered water   |
| VIS 3-5 | tree-covered land: tropical rainforest, deciduous forest, woodland  |
| VIS 6-8 | "short" vegetated land: shrubland, grassland, tundra  |
| VIS 9   | desert  |
| VIS 10  | ice-covered land  |
| VIS 11  | snow-covered land or within 100 km of snow regardless of permanent vegetation classification  |

Radiance Angle Corrections

To compare radiances observed at different times, corrections must be made to reduce radiance variations caused by changes in satellite viewing geometry or solar illumination geometry. The main procedure is to make all time comparisons independently for each 3-hr interval of the day (i.e., constant diurnal phase), so that variations of solar geometry and diurnal variations in surface temperature are minimized within one month (variations of actual image time of up to 1.5 hours about the nominal time can occur). The satellite viewing geometry is actually nearly constant for each location in geostationary satellite images. The polar orbiter observations, though nominally sun-synchronous, actually have varying viewing and solar illumination geometries, but the range of angles at each location is limited. Thus, the remaining geometry variations of the radiances are small and can be removed accurately enough by simple transformations.

For the IR, the radiances (as brightness temperatures) are corrected to a nadir view using

$$T(1) = T(\mu) + C_0(\mu) + C_1(\mu) [ T(\mu) - 250 ]$$

$$C_0(\mu) = - (1.93 + 2.520\mu) (1/\mu - \mu) / 4.8$$

$$C_1(\mu) = (0.267 + 0.053\mu) (1/\mu - \mu) / 4.8$$

where  $\mu$  is the cosine of the satellite zenith angle and the numerical coefficients were derived by a best fit to radiative transfer model calculations using a global distribution of seasonal mean TOVS temperatures and humidities. The factor  $(1/\mu - \mu)$  is the function used to interpolate between two brightness temperature values; the extra factors involving  $\mu$  arise because the correction procedure must approximate the dependence on  $T$  (first atmospheric level) and the surface temperature by using the observed brightness temperature,  $T(\mu)$ . The radiative model is the same one used later in the analysis of the satellite IR radiances (Section 3.2.5). This formula fits all the data to within about 1-2 K. Since the polar orbiter data are limited to  $\mu > 0.45$ , the errors in using the same formula for all latitudes and seasons are actually  $\leq 1$  K.

For the VIS, the radiances are corrected to nadir sun using

$$R(\mu_0) = \mu_0 R(1)$$

where  $\mu_0$  is the cosine of the solar zenith angle and is the value for the actual image **pixel** time and location. This correction neglects the weak anisotropy of land surface reflectances and the  $\mu$ -dependence of Rayleigh scattering and ozone absorption, which partially offset each other. Tests of the errors introduced by neglecting these effects show that they are  $\leq 0.01$ - $0.02$  (absolute) for the range of geometries encountered by the polar orbiter at any one location. Only the very dark water surfaces are affected noticeably by this approach; however, we compare the resulting clear VIS radiances to a water reflectance model to eliminate cloud contamination, so that this effect is also removed. The corrected values are true reflectances only for the sun at the mean sun-Earth distance.

### Tests for Clear Conditions

The first pass through the B3 data tests the spatial variability of the IR radiances within small regions (about 100 km over land and 300 km over water). This test is performed in the original satellite image coordinates for convenience. All pixels determined to be colder (by 3.5 K over water and 6.5 K over land) than the locally warmest pixel are labeled CLOUDY; all others (including the warmest) are labeled UNDECIDED.

The radiance images are then corrected for viewing geometry effects and mapped onto fixed map grids with a resolution approximating the nadir resolution of the original images (25 km). The second pass through the B3 data then tests the time variability of the IR radiances over three days at the same time each day (each UTC is tested separately over the whole month). All pixels determined to be colder (by 3.5 K over water and 8.0 K over land) than the values at the same location on the previous or following day are labeled CLOUDY; all pixels found to have a similar temperature (to within 1.1 K over water and 2.5 K over land) as they have on the previous or following day are labeled CLEAR. The remaining pixels with intermediate variability are labeled UNDECIDED. On some occasions, the test result for one direction in time will conflict with the result in the other direction; if the conflict is strong (i.e., CLOUDY and CLEAR are determined), these cases are labeled MIXED. The UNDECIDED result is not considered a strong conflict.

The final classification of the IR radiance for each pixel is determined by the following logic (Figure 3.7):

|                  |  | SPACE TEST RESULT |           |
|------------------|--|-------------------|-----------|
| TIME TEST RESULT |  | CLOUDY            | UNDECIDED |
| CLOUDY           |  | CLOUDY            | CLOUDY    |
| UNDECIDED        |  | CLOUDY            | UNDECIDED |
| MIXED            |  | MIXED             | MIXED     |
| CLEAR            |  | MIXED             | CLEAR     |

**Figure 3.7.** Space-Time classification logic.

### Clear Sky Statistics - IR

From the classified data, several statistics are collected over 5-day periods at each UTC, separately, to be used in the IR clear sky composite tests:

- (i) the number of CLEAR observations, NCLEAR, in a spatial domain, centered on each pixel and including its nearest neighbors (a region about 75 km in size),
- (ii) the average IR brightness temperature, TAVG, for all CLEAR observations in this domain, and
- (iii) the two largest values of IR brightness temperature, TMAX1 and TMAX2, for all observations in this domain.

If  $TMAX1 - TMAX2 > 12$  K for any individual 5-day interval, then  $TMAX = TMAX2$ ; otherwise  $TMAX = TMAX1$ . The 5-day values of NCLEAR, TAVG and TMAX are the short-term values (NCLEAR-ST, TAVG-ST and TMAX-ST) and are used to calculate long-term values (NCLEAR-LT, TAVG-LT, and TMAX-LT). For surface Type 1 (open water), short-term is taken to be 15 days and long-term is 30 days; for surface Types 2, 3, and 4, short-term is 5 days and long-term is 15 days. If the total number of observations available in a 5-day interval is less than 15, the comparison of TMAX1 and TMAX2 is not performed; if the total number of observations is less than 3 in a 5-day interval, then no clear sky analysis is performed at all for that location.

Because of slow seasonal trends of surface temperature, TMAX for one month may be biased towards the earlier or later part of the month. To correct for this effect, the modes of the differences between the two 15-day values of TMAX in each  $2.5^\circ$  latitude zone for each surface type are used to calculate a linear trend correction to TMAX for each 5-day period in the month. This correction is performed only if the number of pixels in each latitude zone for a given surface type is  $> 300$  and if the fraction of the total number of pixels that have different values of the two TMAX values is  $\geq 65\%$ .

### Clear Sky Statistics - VIS

For each daytime pixel, the value of RMIN is calculated from all the VIS radiances for each 5-day period (RMIN-ST) and for a 30-day period (RMIN-LT); RMIN is calculated for 5-day and 15-day periods poleward of 50° latitude. If any nighttime data are found in the record within the 30-day (or 15-day) period for a particular pixel, no RMIN value is reported and the classification of that pixel is changed to "nighttime" for all days within the month.

### Clear Sky Compositing - IR

Intercomparison of all the pixel statistics determines the estimate of the clear radiance for each pixel every five days, separately at each diurnal phase. These radiance values are called the clear sky composite; the comparison logic is illustrated in Figure 3.8.

The IR clear sky compositing logic assumes that the relatively small variations of surface temperatures (at constant diurnal phase) and their (almost global) tendency to be larger than cloud temperatures produce a characteristic shape of the warmer part of the IR radiance distribution that varies with surface

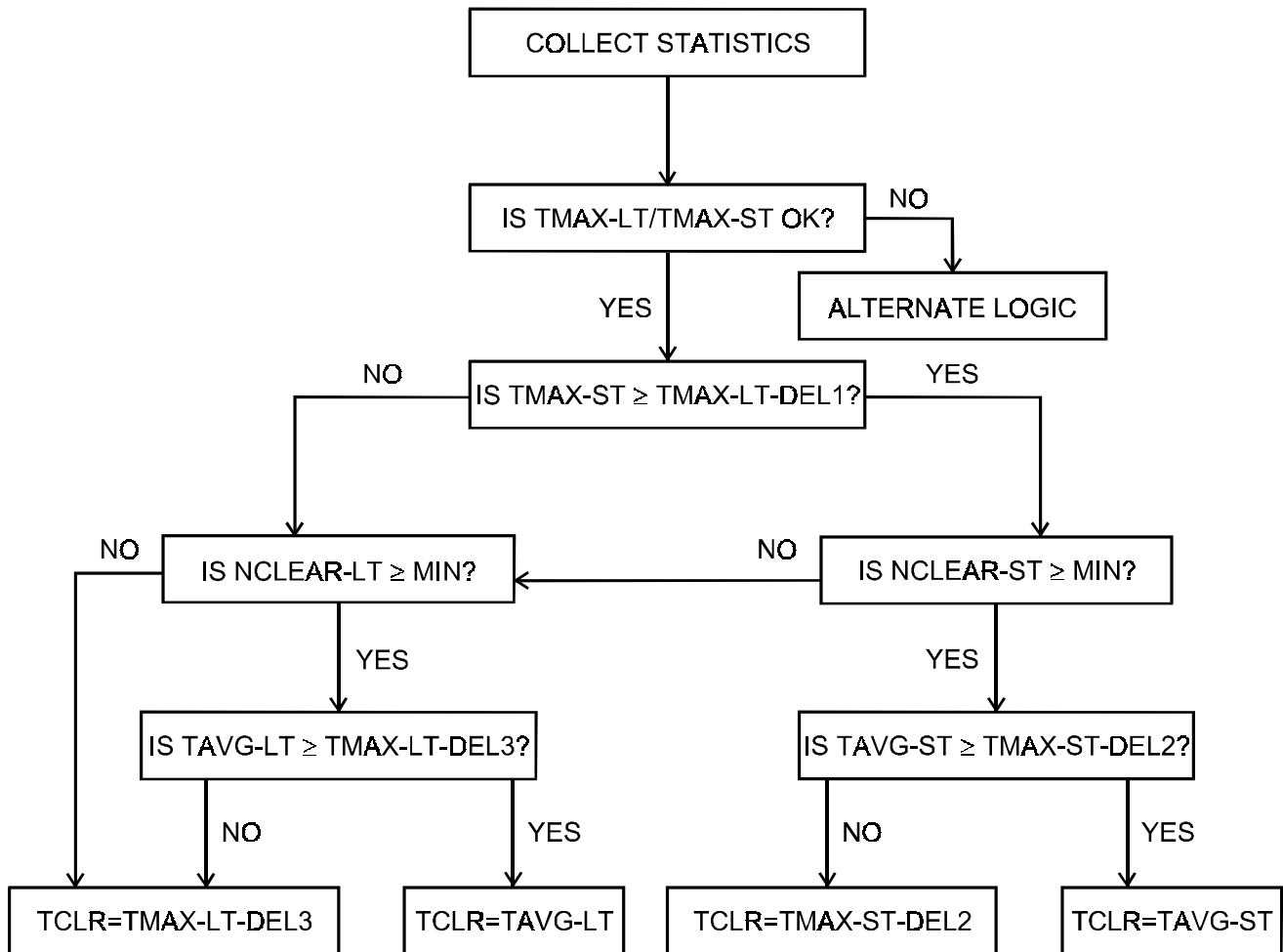


**Figure 3.8.** Infrared clear sky radiance compositing logic.

type (Seze and Rossow 1991a, Rossow and Garder 1993a). The composite logic tests the shape of the IR radiance distribution using the differences between TMAX-LT and TMAX-ST and between TMAX and TAVG (either short- or long-term). If the differences exceed their specified magnitudes, this is interpreted to indicate cloud contamination of one or more of these quantities. Cloud contamination is assumed to decrease over larger time intervals. An additional use of this shape assumption is to reduce TMAX values, whenever they are used for the clear radiance, to approximate the TAVG values, using the assumed maximum difference between TMAX and TAVG.

Five situations may occur.

- (i) The pixel is partially cloudy but the cloudy-clear contrast is very low or the cloudiness is complete and constant with cloudy radiances that exhibit little space *and* time variability.
- (ii) The pixel is mostly cloudy and the cloudy-clear contrast is relatively small, but still larger than the variability of the surface, or cloud persistence and extent are large but not total.
- (iii) The pixel is mostly cloudy but the cloudy radiances exhibit relatively large variability in space and/or time.
- (iv) The pixel is partly cloudy (spatially) or almost totally cloudy occasionally and the cloudy-clear contrast is relatively large.
- (v) The pixel is relatively clear.

The first and last case resemble each other in that the magnitude of the cloudy radiance variability in case 1 is similar to that in case 5 or the cloud cover is complete for 30 days with little variation in cloudy radiances. If this resemblance is strong enough, there is no way to detect such clouds using satellite data alone (see discussion in Rossow and Garder 1993a).

In case 2, either the radiance variations caused by cloudiness are relatively small or almost no observation represents completely clear conditions. This is indicated by the fact that  $TMAX-LT > TMAX-ST + DEL1$  and  $TAVG-LT + DEL3$ , in which case the estimate of clear radiance is  $TCLR = TMAX-LT - DEL3$  (see Table 3.2.2 for values of DEL1, DEL2, DEL3 and DEL4). The value of TMAX-LT used has been corrected for any zonal mean trend over the month. The larger variability of land surface temperatures makes this test much less effective over land than it is over water.

In case 3, in contrast to case 2, the cloudy radiance variability is large enough that the space/time tests detect the clouds. That the location is mostly cloudy is indicated by a very low NCLEAR value. If this condition persists for most of the 30-day period ( $NCLEAR-LT < 10\%$ ), then the estimate of  $TCLR = TMAX-LT - DEL3$ , where TMAX-LT is for 30-days, even for surface Types 2, 3, and 4. If the condition only occurs on the short-term ( $NCLEAR-LT \geq 10\%$ ), then the estimate of  $TCLR = TAVG-LT$ . In both case 2 or 3 (when the long-term information is used for TCLR), the consistency of the result is maintained by ensuring that the value of TCLR obtained is  $\geq TMAX-ST - DEL2$ . This test is more effective over land than over ocean.

In case 4, while there are enough CLEAR values available on the short-term, there is still enough cloud contamination that  $TMAX-ST > TAVG-ST + DEL2$ , in which case  $TCLR = TMAX-ST - DEL2$ .

In case 5, the CLEAR values provide an accurate measure of the clear radiances; the best estimate for the whole 5-day period is  $TCLR = TAVG-ST$ .

**Table 3.2.2. Radiance Difference Values Used in IR Clear Sky Composite Tests.**

| SURFACE TYPE<br>(Table 3.2.1) | DEL1 | DEL2 | DEL3 | DEL4 |
|-------------------------------|------|------|------|------|
| 1                             | 2.0  | 2.0  | 2.5  | 4.0  |
| 2                             | 4.0  | 3.0  | 4.0  | 6.0  |
| 3                             | 6.0  | 5.0  | 8.0  | 8.0  |
| 4                             | 9.0  | 7.0  | 11.0 | 10.0 |

Since the compositing tests rely on the relationships with TMAX values, some protection is required to prevent false results because of a few spurious data values that occasionally represent very large temperatures. The protection procedure compares the value of TMAX-LT for each pixel against the regional distribution of these values: if the particular TMAX-LT - DEL4 > the regional modal value **and** its corresponding TAVG-LT, then this value is replaced using the regional distribution. If a value of TMAX-LT is determined to be too large by this procedure, any value of TMAX-ST that is too close to TMAX-LT is also avoided. In practice this procedure is not very successful, so it is augmented by the 5-day TMAX test described above; and consequently, it is very rarely invoked.

A spatial filter was applied in the old analysis procedure (Rossow and Garder 1993a), but it has been eliminated from the new procedure.

#### Clear Sky Compositing - VIS

The VIS clear sky compositing logic (Figure 3.9) assumes that the small variations of surface reflectance (at approximately constant viewing and illumination geometry) and their almost global tendency to be smaller than cloud reflectances produce a characteristic shape of the darker part of the VIS radiance distribution (Sèze and Rossow 1991a, Rossow and Garder 1993a). Time variations for surface reflectances for most surface types are generally much smaller than the spatial variations. The relatively simpler time/space behavior of surface reflectances allows use of a simple statistic: the minimum VIS radiance over a sufficiently long time period to insure that clear conditions occur. However, this approach does bias the actual clear radiance value (Matthews and Rossow 1987, Rossow *et al.* 1989), so the same shape assumption is used to increase the minimum value by an amount representing the typical separation of the minimum and the mean value.

The eleven surface types (Table 3.2.1) are grouped into five categories: (1) variable water, (2) rapidly time-varying land, (3) temporally constant, spatially heterogeneous land, (4) constant water, and (v) spatially/ temporally constant land.

- (1, 2) Variable water and rapidly varying land are determined by the presence of sea ice cover and snow cover, respectively (permanently ice covered land is treated as snow covered land). These two surfaces also have reflectances that are more nearly the same as those of clouds, so that the VIS radiance contrast is low. The clear radiance  $RCLR = RMIN-ST + DEL1$ .
- (3) Some locations exhibit relatively large spatial variations of surface reflectance but small time variations (Sèze and Rossow 1991a): these types are high topography regions (because of stronger solar zenith angle dependence and shadowing effects), deserts, tundra, and grasslands.  $RCLR = RMIN-LT + DEL2$ .

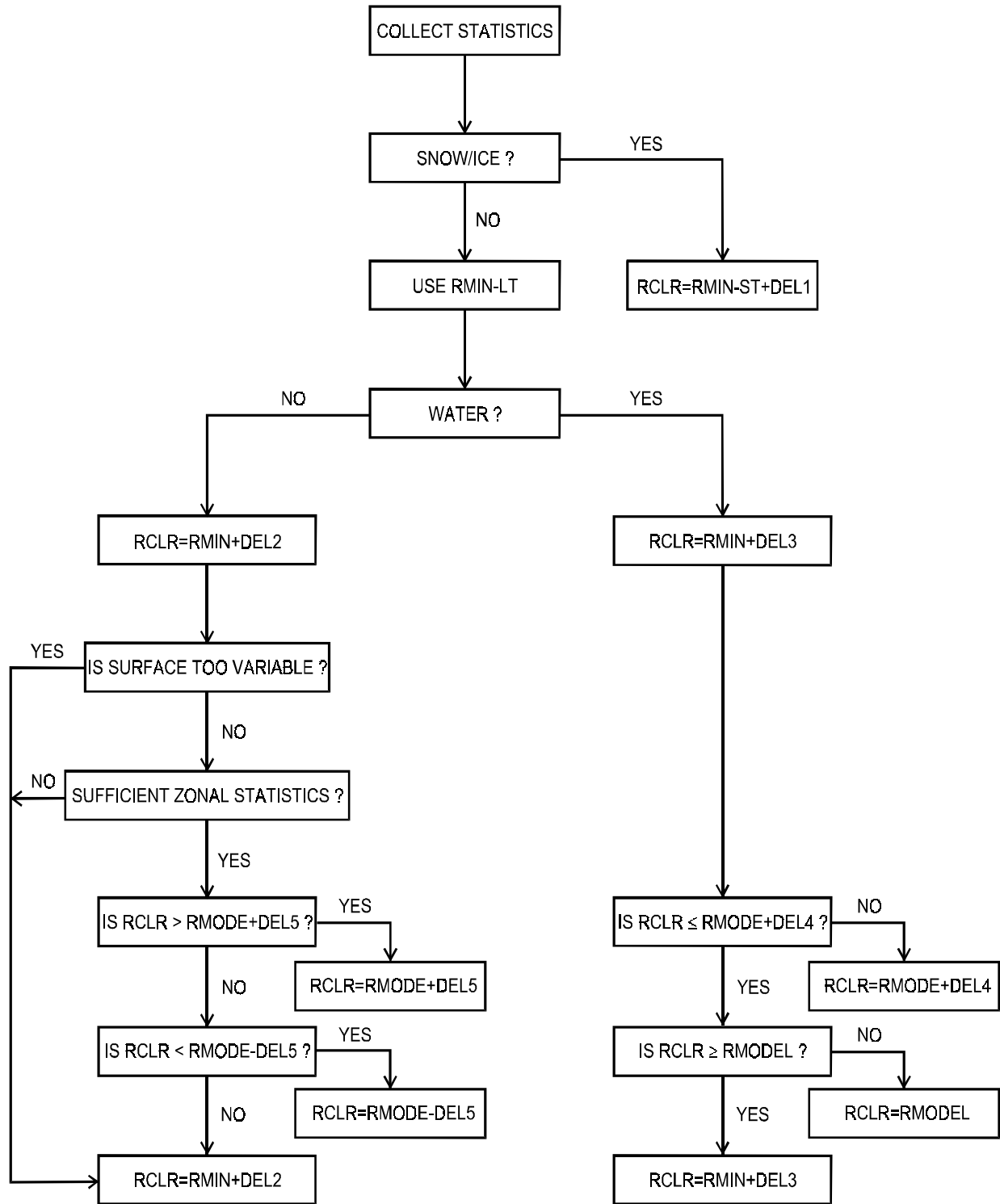


**Figure 3.9.** Visible clear sky radiance compositing logic.

- (4) Open water generally exhibits constant reflectance in time and space at constant viewing/illumination geometry; however, since the viewing/illumination geometry for satellites varies (especially for the polar orbiter), the observed reflectance varies more because of the strong anisotropy of the surface. In particular, the reflectance of sun glint is highly variable because of the variation of surface roughness with surface winds.  $RCLR = RMIN-LT + DEL3$ . This value is not allowed to deviate from an empirical model of water VIS reflectance (derived from the model of Minnis and Harrison 1984). The model includes an additional augmentation for glint conditions. For a conservative estimate of the reflectance,  $RMODEL + DEL4 \geq RCLR \geq RMODEL$ .
- (5) The surface types that are spatially as well as temporally homogeneous are vegetated land surfaces: shrubland, woodland, forest and tropical rainforest.  $RCLR = RMIN-LT + DEL2$ ; however, the individual values are compared to the distribution of values for the same surface type in  $10^\circ$  latitude zones and are required to meet the condition:  $RMODE + DEL5 \geq RCLR \geq RMODE - DEL5$ .  $RMODE$  is the peak value of the distribution. If  $RCLR$  for a particular pixel is outside the range, it is re-set to the nearest value in the range.

The DEL values in scaled radiances are:  $DEL1 = 0.050$ ,  $DEL2 = 0.035$ ,  $DEL3 = 0.015$ ,  $DEL4 = 0.030$  and  $DEL5 = 0.060$ .

#### First Clear sky radiances

The clear sky composites are constructed for every pixel for every 5-day period. Note, however, that the IR clear sky composite procedure uses some nearest-neighbor information; thus, the effective spatial resolution of the IR composite is about 75 km. The composite radiances have had the viewing geometry dependence removed before compositing, so in the threshold step the nearest-in-time clear sky composite is selected and the **inverse** angle corrections applied, using the specific viewing geometry for each pixel in that image. Thus, although the values in the clear sky composites are held constant over 5-day periods, the clear radiances used to detect clouds can undergo some day-to-day variation as viewing geometry varies.

Glint geometry over water is determined by the magnitude of the solid angle between the specularly reflected solar illumination vector direction (the outgoing direction not the incoming direction) and the actual satellite view vector direction. The reflected solar vector direction is defined by the solar zenith angle,  $\theta_0$ , where  $\mu_0 = \cos(\theta_0)$ , and a position azimuth angle; the satellite view vector is defined by the satellite zenith angle,  $\theta$ , where  $\mu = \cos(\theta)$ , and another position azimuth. In radiative transfer applications, the relative azimuth angle,  $\phi$ , is defined as  $180^\circ$  minus the difference of the usual position azimuth angles. Thus, the solid angle,  $\alpha$ , between these two vector directions is given by

$$\cos(\alpha) = \cos(\phi) [ \cos(\theta_0) \cos(\theta) + \sin(\theta_0) \sin(\theta) ]$$

Glint conditions are defined by  $\alpha < 30^\circ$ . An empirical model of water reflectance replaces the clear sky composite values in glint conditions. The model is based on a four month (one from each season) survey of clear sky radiances from the C-series cloud analysis for geostationary and polar orbiting satellite

### 3.2.4.2. FIRST CLOUD DETECTION THRESHOLDS

The status of each individual pixel, CLOUDY or CLEAR, is decided by threshold tests for each spectral radiance, independently and without regard to the labels previously assigned in the clear sky composite analysis. In order to improve the detection of cirrus and low-level clouds, single channel detections are allowed. Thus, using the clear sky radiances derived for each location and time, any pixel with **any** radiance value that is sufficiently different from the corresponding clear sky radiance is declared to be CLOUDY. The magnitude of the difference required (called the threshold) is set by the estimate of the uncertainty in the clear radiance values. All remaining pixels are called CLEAR.

The success of the overall cloud detection is indicated by whether the clear sky composite analysis and threshold labels generally agree or not (Rossow and Garder 1993a): more than 90% of pixels labeled as cloudy or clear in the clear sky composite analysis are similarly labeled by the threshold decision. The pixels in the undecided category are usually divided into cloudy and clear in rough proportion to the number of pixels already labeled as cloudy or clear.

The magnitudes of the thresholds vary with the IR surface types defined on page 61, but sea ice is treated as Type 3 for VIS. Note that the VIS threshold test is performed, **not on reflectances, but on radiances**, which are represented as fractions of the instrument response obtained when measuring the full solar flux. IR radiances are represented as brightness temperatures in Kelvins. The threshold values used are:

**Table 3.2.3. First Cloud Detection Threshold Values.**

| RADIANCE | SURFACE TYPES (Table 3.2.1) |      |      |      |
|----------|-----------------------------|------|------|------|
|          | 1                           | 2    | 3    | 4    |
| IR (K)   | 2.5                         | 4.0  | 6.0  | 8.0  |
| VIS      | 0.03                        | 0.03 | 0.06 | 0.06 |

In the old version of the cloud detection algorithm, there were a few specific exceptions to these threshold values, but these have been eliminated in the new version. The most important difference that this introduces is to reduce the effective VIS threshold over snow and ice surfaces from 0.12 to 0.06.

### 3.2.4.3. FINAL CLEAR SKY RADIANCES

In the old cloud detection procedure, the above threshold tests of the IR and VIS radiances (only IR at night) were the last step. In the new cloud detection procedure, there are two additional steps. In the third step, some small refinements are made to the clear radiances based, in part, on the results of the first threshold tests. In addition in polar orbiter data (from AVHRR), radiances measured at 3.7  $\mu\text{m}$  are processed, using the results of the first threshold step, to obtain clear sky composites: in daytime the thermal emission contribution is removed to obtain composite solar reflectivities and at night the composite difference of 3.7  $\mu\text{m}$  and IR brightness temperatures is obtained.

## IR Clear Sky Refinements

The results of the first two steps for a whole month are examined several times at each time of day UTC, separately. The first pass through the data identifies the two largest brightness temperatures (called TMAX1 and TMAX2) for each pixel and classifies each pixel into one of five types (note that these five types differ from the four types used in the first clear sky analysis - see Table 3.2.1):

Type 1 = near-coast land and water, high topography if not covered by ice

Type 2 = open water, water that is in the margin zone near sea ice or covered by sea ice for only part of the month

Type 3 = water fully covered by sea ice all month

Type 4 = open land, land that is in the margin zone near snow or covered by snow for only part of the month

Type 5 = land covered by snow all month, land ice

In the second pass, a HOT flag is set for each pixel where  $TMAX1 - TMAX2 > 10$  K, except for Type 1. In a third pass, the neighboring pixels in a 5x5 domain around each flagged pixel are checked to see whether any unflagged pixel in the same class has a TMAX value larger than the flagged value. If so, the flag for the center pixel is turned off.

The fourth pass through the dataset re-creates (with angle corrections made) the complete 5-day IR clear sky radiance maps for each UTC, separately, that resulted from the first part of the cloud analysis. In addition, flags are set for each pixel indicating which short-term or long-term statistic (TAVG-ST, TMAX-ST, TAVG-LT, TMAX-LT) was used for the original clear sky radiance (see Section 3.2.4.1). Results from the old cloud analysis indicated that the values of DEL2 and DEL3 separating short-term and long-term TMAX and TAVG for land pixels, respectively, were too large. Hence, the IR clear sky radiances for snow-free land pixels are increased by 1.0 K when TMAX-ST was used and by 1.5 K when TMAX-LT was used; the clear sky radiances are increased by 2.0 K for snow-covered land when TMAX-LT was used.

Next, three procedures are applied to each 5-day map to correct for spuriously large IR brightness temperature values (TCLR), to correct for the effects on TCLR near coast lines of errors in image navigation, and to correct for some cases of residual cloud contamination. The first procedure reads each map, together with the values of TMAX1 and TMAX2 collected over the whole month for each corresponding location. All pixels that are not Type 1 and do not have the HOT flag set are tested: if  $TCLR > TMAX1 + 1.0$  K, then the HOT flag is set. A 5x5 domain around each pixel with a HOT flag set and TCLR greater than the average of TMAX1 and TMAX2 is searched for all values of TCLR in the same type without a HOT flag set. If at least two such neighbors are found, then the flagged value of TCLR is replaced by the average TCLR of all these neighbors and the flag turned off. If insufficient neighbors are found, nothing is done.

The second procedure searches each clear sky map for unflagged land or open water pixels that are within 75 km or 50 km of a coastline, respectively. A 7x7 domain about each target pixel is examined

for unflagged pixels that are the same type, land or water, as the target. If any sea ice is found within the domain, this procedure is skipped. The average TCLR values are calculated for the pixels of the same type, TSAME, and for the pixels of the opposite type, TOPP, as long as at least two unflagged values are available. If there are insufficient values available, the procedure is skipped. If the absolute value of  $TSAME - TOPP$  is  $> 6.0$  K, there is a strong contrast of clear sky brightness temperature at the coast. If, in addition, the target pixel TCLR differs from TOPP by no more than  $\pm 2.5$  K, this is assumed to mean that the "opposite" type has contaminated the clear sky map because of navigation errors in locating the coastline, so a flag is set for the target pixel. Once all pixels have been examined, flagged values of TCLR are replaced by TSAME and flags turned off.

The third procedure examines  $3 \times 3$  and  $5 \times 5$  domains around each pixel (except Type 1 pixels); if any neighboring pixel is Type 1, a different land/water category or a different snow/ice category than the center pixel, nothing is done. For homogeneous regions with at least three neighbors in either the  $3 \times 3$  domain or the  $5 \times 5$  domain, the spatial variance of the TCLR values is calculated. If a variance is available and it exceeds 0.6 K over open water or 7.6 K over land, then the smallest TCLR value is flagged as COLD. Once flags have been set, the flagged TCLR values are replaced by the average TCLR of any unflagged neighbors.

### VIS Clear Sky Refinements

The results of the first two steps for a whole month are examined several times at each time of day UTC, separately. The first pass collects for each UTC, separately, the two lowest VIS radiances for each pixel, RMIN1 and RMIN2. The second pass re-creates (with angle corrections made) the 5-day VIS clear sky radiance maps for each UTC that resulted from the first part of the cloud analysis. In the third pass, the original VIS clear sky radiance, RCLR, for each pixel is compared with RMIN1 and RMIN2 in different ways depending on the cloudy fraction of the pixels in a  $5 \times 5$  domain centered on that pixel. In the case of smaller cloud amounts, disagreement among these values is interpreted to be caused by cloud shadows that cause the RMIN values to underestimate the proper VIS clear sky radiance, particularly over more reflective surfaces. In the case of larger cloud amounts, disagreements are interpreted as cloud contamination of the RMIN values. This comparison is not performed in the polar regions (latitudes poleward of  $50^\circ$ ), for ice or snow-covered pixels, or for water pixels in sunglint geometry. For sunglint open water, the clear sky radiances are replaced by a revised empirical model. If cloud fraction is  $< 0.80$  and  $RMIN2 - RMIN1 > 0.05$ , then if the corresponding value of  $RCLR < RMIN2$ , RCLR is replaced by RMIN2. If cloud fraction is  $\geq 0.80$  over ocean and RCLR is more than 0.03 larger than the average of RMIN1 and RMIN2, then RCLR is replaced by the average plus 0.03. If cloud fraction is  $\geq 0.80$  over land and  $RCLR \geq RMIN1 + 0.03$ , RCLR is replaced by RMIN1.

### NIR Clear Sky Radiances (polar orbiter data only)

Radiance data from the AVHRR on the NOAA polar orbiters are obtained at additional wavelengths besides IR and VIS. To improve detection of low-level clouds in the polar regions, additional tests have been added to the cloud detection procedure using  $3.7 \mu\text{m}$  radiances (called NIR). At night, the radiances at this wavelength are thermal infrared emission. During daytime, the radiances at this wavelength are dominated by reflected sunlight; but some thermal emission is included. Because the signal-to-noise ratio at this wavelength can be low, a statistical check is performed for each image, separately for each UTC (polar orbiter data is also segmented into three geographic regions, north and south polar and low latitudes, so separate statistics are checked for each region). All NIR radiances are

collected into a frequency histogram for each image (all brightness temperatures < 222 K are excluded). If the histogram has less than 1000 pixels or any single brightness temperature occurs more than 15% of the time, then no further use is made of the NIR radiances for that image. To construct clear sky maps, a whole month of data is analyzed for each time-of-day UTC, separately.

For **nighttime** images a frequency histogram of the difference between NIR brightness temperature (TNIR) and IR brightness temperature (TIR) in Kelvins is collected for pixels labeled as clear by the first IR threshold tests. Radiances from pixels for which TNIR < 222 K or TIR < 230 K are excluded. Histograms are produced for four surface types: open water, all other water, open land, and all other land. The mode value in each histogram is determined. If the histogram is composed of less than 5000 pixels, if the mode value is < -11 K or > 9 K, or if there is a secondary mode value separated from the first by more than 10 K, no further NIR tests are made. Valid mode values represent the clear sky values of the NIR and IR brightness temperature difference, which is nearly zero for most surfaces at high latitudes where atmospheric effects are weak.

For **daytime** images all NIR radiances in pixels determined to be clear by the first IR and VIS threshold tests and with TNIR ≥ 222 K and TIR ≥ 230 K are converted to top-of-atmosphere reflectances (at mean sun-Earth distance):

$$RNIR = (RAD_3 - RAD_4) / (\mu_0 S_3)$$

where RAD<sub>3</sub> is the observed radiance (energy) in the instrument bandpass at 3.7 μm, RAD<sub>4</sub> is the radiance at 3.7 μm produced by a black-body with a physical temperature equal to the observed brightness temperature at 11 μm, and S<sub>3</sub> is the amount of sunlight in the instrument bandpass at 3.7 μm reflected from a surface with unit reflectivity. The two lowest values of RNIR are collected for each pixel, except those with a BAD quality flag. Clear sky values for RNIR are determined as the average of the two lowest values, if they are available for that pixel, and, if they are not available, the clear sky value is the average over other pixels in the same land/water category in a 5×5 domain centered on that pixel. The clear sky values of RNIR are then increased by 0.02 for all surface types, except open land for which they are increased by 0.03.

#### 3.2.4.4. FINAL THRESHOLDS

The final new part of the cloud detection procedure (fourth step) is to repeat the threshold tests using the final clear sky radiances with three changes: the IR thresholds for land surfaces (Types 3 and 4) are reduced by 2.0 K, the VIS threshold test is changed to a test of **reflectance** values instead of **radiance** values and a NIR threshold test is added over ice and snow-covered surfaces only. A pixel is labeled cloudy if **any** observed radiance differs from the corresponding clear sky value for that pixel by more than the threshold values given in the Table 3.2.4. The label is assigned without regard for the results of previous tests. For the IR test, the four surface types are: Type 1 = open water, Type 2 = near-coastal water, sea ice margin and sea ice, Type 3 = open land, and Type 4 = near-coastal land, high topography, snow margin, and snow and ice-covered land. For the VIS and NIR tests, the same four surface types are used, except that sea ice margin and sea ice are changed to Type 3. The only special exception is that the VIS threshold test is not performed in sunglint geometry over open water.

**Table 3.2.4. Final Cloud Detection Threshold Values.**

| WAVELENGTH         | SURFACE TYPES |       |       |       |
|--------------------|---------------|-------|-------|-------|
|                    | 1             | 2     | 3     | 4     |
| IR (K)             | 2.5           | 3.5   | 4.0   | 6.0   |
| VIS Reflectance    | 0.030         | 0.030 | 0.060 | 0.090 |
| VIS Radiance Limit | 0.025         | 0.025 | 0.040 | 0.040 |
| TNIR (K)           | 8.0           | 8.0   | 8.0   | 8.0   |
| NIR Reflectance    | 0.045         | 0.045 | 0.055 | 0.055 |

Since a constant **reflectance** threshold represents progressively smaller **radiance** differences as solar zenith angle increases ( $\mu_0$  decreases), the threshold can decrease to values smaller than the uncertainties in the measured radiances or the inferred clear sky radiances. To avoid this, the VIS threshold test is actually performed as a radiance test, where the *radiance* threshold is equal to the values given in Table 3.2.4 multiplied by  $\mu_0$  for that pixel at that time, as long as the value is greater than or equal to the corresponding limit given in the table.

At night TNIR is nearly equal to TIR for clear pixels, but differs significantly in both the positive and negative directions for some clouds. Thus, the threshold test on TNIR labels a pixel cloudy if the absolute value of the difference,  $|TNIR - TIR|$ , is larger in magnitude than the values given in Table 3.2.4. Before the test, an adjustment is made to the value of  $TNIR - TIR$  based on the mode value of a frequency histogram of all clear values of  $TNIR - TIR$  collected for the whole month over open water and land. This adjustment compensates for any changes in relative calibration between the two wavelength channels. The difference values are also constrained to be  $\geq -18$  K and  $\leq 25$  K; values outside this range are considered clear. During the daytime, the RNIR threshold test is similar to the VIS threshold test: the observed value of RNIR (as long as  $TNIR - TIR > -17$  K) is compared to the clear sky composite value and the pixel labeled cloudy if RNIR is greater than the clear sky value by more than the values given in Table 3.2.4 (there is no lower limit because the sensitivity of this channel and the threshold magnitudes are large enough to avoid loss of precision).

### 3.2.5. RADIATIVE TRANSFER MODEL ANALYSIS

Once pixels are classified as cloudy or clear, the radiances are compared to radiative transfer model calculations designed to simulate the measurements of the AVHRR channels (to which all the radiometers have been normalized). Note that the model simulates **spectral radiances**; that is, the model calculates the full angular variation of radiant intensity over finite spectral intervals at particular wavelengths as functions of the physical properties of the clouds, atmosphere and surface. Comparison of observed radiances to simulated radiances are used to retrieve the surface reflectances and temperatures from clear radiances and the cloud optical thickness and top temperature from cloudy radiances. Atmospheric properties that affect the satellite measured radiances are specified from correlative data.

For the C-series of the cloud products, the VIS and IR absolute calibrations were referenced to the AVHRR on NOAA-7 (Brest and Rossow 1992). For the D-series of the cloud products, the VIS and IR absolute calibrations are referenced to that of the NOAA-9 AVHRR, which has been calibrated by

aircraft instruments (Rossow *et al.* 1996). The new VIS and IR calibrations are estimated to be accurate to within  $\pm 7\%$  and  $2\%$ , respectively.

The radiative model analysis proceeds in five steps (Figure 3.10).

- (1) Retrieval of surface temperature, TS, from the clear IR radiance obtained from the IR clear sky composite for the particular image pixel. The effects of atmospheric water vapor absorption are removed, using the atmospheric data for the particular location and time. A new formulation of the water vapor continuum absorption is used for the D-series of the cloud products.
- (2) Retrieval of surface reflectance, RS, from the clear VIS radiance obtained from the VIS clear sky composite for the particular image pixel. A correction for varying sun-Earth distance is made and the effects of Rayleigh scattering and ozone absorption are calculated, using ozone abundance data for the particular location and time. No aerosol effects are included and no retrieval is performed at night.
- (3) Retrieval of TS from the observed IR radiance, if the pixel is labeled CLEAR, or retrieval of cloud top temperature, TC, if the pixel is labeled CLOUDY. All clouds are assumed to be opaque to IR radiation. The effects of atmospheric water vapor absorption are removed, using the atmospheric data for the particular location and time. A new formulation of the water vapor continuum absorption is used for the D-series of the cloud products. Cloud top pressure, PC, is inferred from the atmospheric temperature profile for the particular location and time.
- (4) Retrieval of RS from the observed VIS radiance, if the pixel is labeled CLEAR, or retrieval of cloud optical thickness, TAU, if the pixel is labeled CLOUDY. The effects of Rayleigh scattering and ozone absorption are calculated; for a cloudy pixel the Rayleigh scattering is calculated, using the cloud top pressure retrieved in Step 3. Calculation of cloud optical thickness also uses the surface reflectance from the VIS clear sky composite, obtained in Step 2 for land and sea ice surfaces or from a model for water surfaces. In the D-series of the cloud products, NIR radiances are used to improve the retrieval of TAU over highly reflective snow and ice surfaces in the polar regions. Optical thickness is retrieved for each cloudy pixel using two cloud microphysical models: the same liquid droplet model used in the C-series of the cloud products and an ice crystal model (results reported only for clouds with top temperatures  $< 273$  K). No retrievals of RS and TAU are done at night.
- (5) If the optical thickness of the cloud is small, the cloud top temperature is adjusted to account for transmission of radiation from the surface using the retrieved optical thickness. The adjusted cloud top pressure is then used to re-calculate the optical thickness. In the D-series of the cloud products, an additional adjustment is also made to account for the small effect of scattering on IR radiances. No adjustment is performed at night.

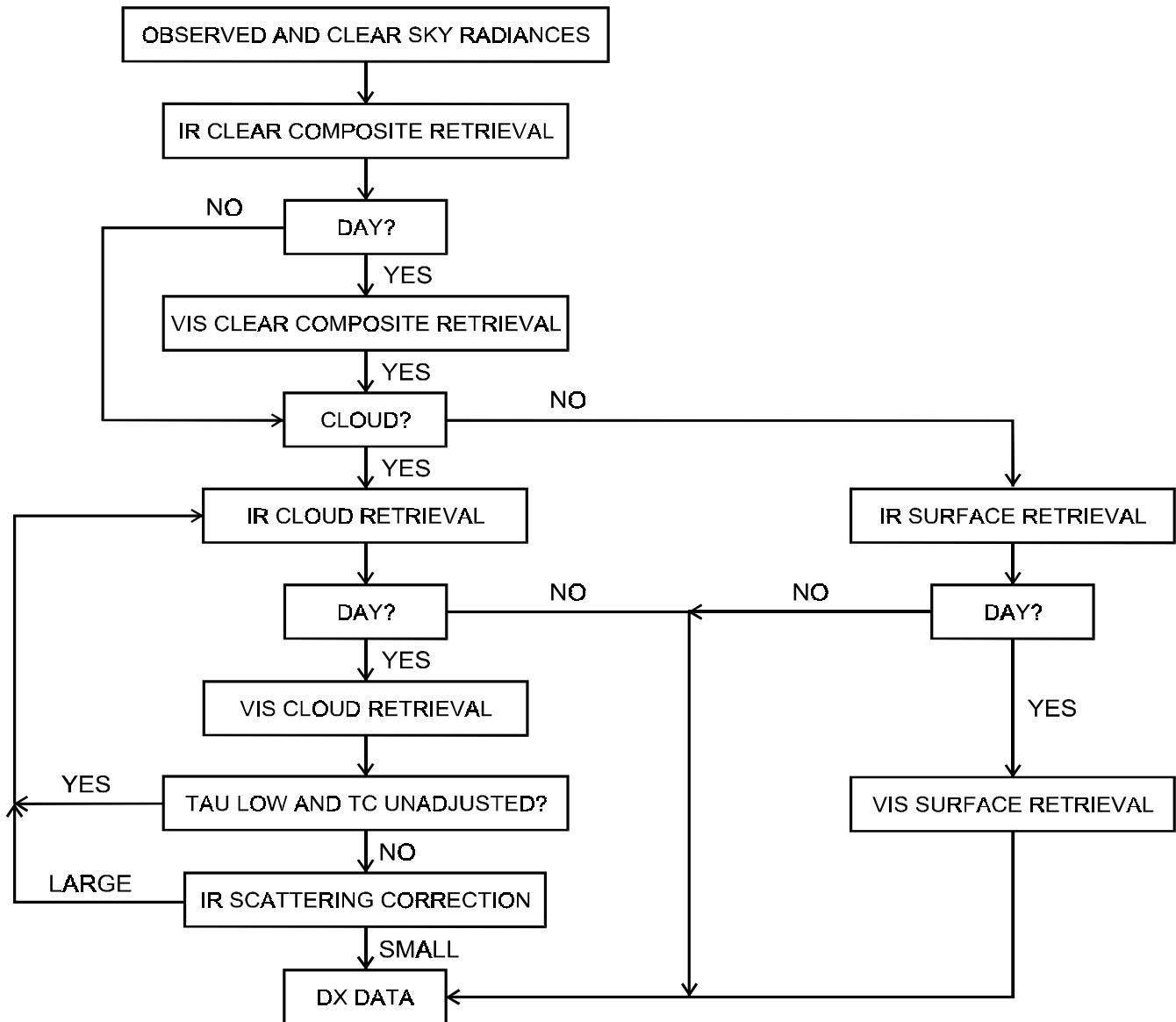


**Figure 3.10.** Radiative model analysis logic.

### 3.2.5.1. RADIANCE MODEL DESCRIPTIONS

All retrieved parameters are model-dependent quantities. The accuracy with which they represent real quantities depends on two factors:

- (i) the extent to which variations of other cloud and surface characteristics, which are held constant in the model, change the radiances, and
- (ii) the importance of effects neglected in the model.

The first of these factors will affect the accuracy of a specific observation, but will not, generally, affect the statistical results (climatology) as long as the estimated values for these parameters are "climatologically" correct. The variations in the satellite-measured radiances that are caused by changes of other cloud properties will be included as variations of optical thickness and top temperature. One important assumption in the model is the microphysical properties of the cloud particles. In the C-series of the cloud products, a specific spherical droplet distribution with an effective radius of  $10 \mu\text{m}$  was used. Subsequent research has shown that this is reasonably close to the global mean value for liquid water clouds ( $\approx 11 \mu\text{m}$ , Han *et al.* 1994). However, spherical particles do not provide a good approximation to ice crystals in high-level clouds (cf., Minnis *et al.* 1993). In the D-series of the cloud products, an ice crystal model, similar to that investigated by Minnis *et al.* (1993), is also employed. Both optical thickness values are reported if the ice model top temperature  $< 273 \text{ K}$ ; only the liquid water value is reported at higher temperatures.

The second of these factors may introduce important biases into these results. The most uncertain issue in this category is the assumption of optical homogeneity (of clouds and surfaces) at pixel spatial scales ( $\approx 5 \text{ km}$ ). One feature of the results that may be related to this issue is a small systematic variation of the retrieved cloud properties with increasing satellite viewing zenith angle (Rossow and Garder 1993b). Research activities continue to address these questions.

The following sections describe the detailed assumptions made about the cloud, atmosphere, and surface characteristics. Key highlights are:

- (1) Surface and atmospheric optical properties are assumed to be uniform over the image pixels (4-7 km, but actually interpreted to be uniform over the mapped cell scale of 25 km).
- (2) No aerosol effects are included in the radiative models; hence, the mean properties of the surface include the climatological effects of aerosols. Variations in aerosols that change the radiances enough in time, particularly dust storms, will be detected as clouds.
- (3) All surface types are assumed to be black bodies in modeling IR radiances; hence, the retrieved temperatures are brightness temperatures that are slightly lower than the actual skin temperatures of the surface. These values will differ from near-surface air temperatures by an amount that varies with time of day and season (see Rossow and Garder 1993b).
- (4) Land and sea ice surfaces are assumed to be isotropic reflectors. The water surface reflectance is represented by an anisotropic model derived from satellite observations (Minnis and Harrison, 1984; see also Rossow *et al.* 1989).
- (5) Cloud optical properties are assumed to be uniform over the image pixels; hence, cloud cover of pixels is assumed to be either zero or one.
- (6) Clouds are assumed to be single, physically thin layers (no vertical temperature gradients) that are strong absorbers of IR radiation. In the D-series of the cloud products, the effects of IR radiation scattering, which are a function of optical thickness, are also included for daytime retrievals.

- (7) Clouds are assumed to be single, thin layers that are pure (conservative) scatterers of VIS radiation. No gaseous absorption or scattering is included in the cloud layer. Scattering in the liquid droplet model is calculated as Mie scattering from a size distribution of water spheres with an effective radius of 10  $\mu\text{m}$  and effective variance of 0.15. In the D-series of the cloud products, scattering in the ice crystal model is calculated using a fractal phase function (Macke 1994, Mishchenko et al. 1996) and a -2 power law size distribution between 20 and 50  $\mu\text{m}$  that has an effective size of 30  $\mu\text{m}$  and an effective variance of 0.1.

### IR Model

The infrared radiance model is very similar to that described in Rossow *et al.* (1989), with optical constants adjusted to the spectral response of Channel 4 on the NOAA-9 AVHRR (see Rossow *et al.* 1992). The model represents the clear atmosphere as seven layers of absorbing gas (the pressure intervals are surface or 1000, 800, 680, 560, 440, 310, 180, tropopause or 30 mb) above a black-body surface; no aerosol effects are included. Each pixel is assumed to correspond to a column of gas with horizontally uniform properties; the surface and any cloud layers are also assumed to be horizontally uniform over the image pixels (4-7 km).

Clear gas layers in the model are not isothermal; rather the gas temperature varies from top to bottom of the layer so that the Planck function is linear (this is equivalent, however, to a nearly linear temperature variation with pressure for the relatively thin layers used). Radiances (brightness temperatures) are calculated as a function of satellite zenith angle. Absorption is due to water vapor; the total amount of water vapor within each pressure layer is vertically distributed with a constant mixing ratio.

Water absorption has two contributions: continuum and weak line absorption. The formulation of the continuum absorption follows that of Ma and Tipping (1991, 1992, 1994) (the previous version of the analysis used the continuum absorption formulation of Roberts et al., 1976) and includes the temperature dependence of both the self-broadening and foreign-broadening effects. The optical thickness of continuum absorption in a specific atmospheric layer with pressure interval  $dP$  is given by

$$\tau_s = (L_0 V_0 / mg) (1.607 AS) dP / (\log AS_b - \log AS_t)$$

$$\tau_f = (L_0 V_0 / mg) (1.607 AF) dP / (\log AF_b - \log AF_t)$$

where  $L_0$  is Loschmidt's number =  $2.68714 \times 10^{19}$  mole/cm $\cdot$ ,  $V_0$  is the molar volume =  $2.24207 \times 10^4$  cm $\cdot$ /mole,  $m = 18$  g/mole is the molecular weight of water,  $g = 980$  cm/s $\cdot$  is the acceleration of gravity, and  $dP$  is the layer pressure interval in mb. The quantities  $AS_t$ ,  $AS_b$ ,  $AF_t$ , and  $AF_b$  are determined for the atmospheric temperatures at the top and bottom of each atmospheric layer by multiplying temperature-dependent coefficients, calculated from the model of Ma and Tipping, by the square of the mass mixing ratio of water vapor for AS and of the rest of the atmosphere for AF. The quantities AS and AF are given by

$$AS = AS_t P_t - AS_b P_b - (AS_b - AS_t) dP / (\log AS_b - \log AS_t)$$

$$AF = AF_t P_t - AF_b P_b - (AF_b - AF_t) dP / (\log AF_b - \log AF_t)$$

The factor of 1.607 is ratio of atmospheric and water molecular weights that converts one factor of mass mixing ratio into a number mixing ratio. This formulation provides an accurate treatment of the

temperature dependence of the water vapor absorption variation over a finite atmospheric layer with vertical variations of temperature and water mixing ratio. If the variation of the AS and AF across a layer is too small, an alternative formula is used that replaces the factors  $AS / (\log AS_b - \log AS_t)$  and  $AF / (\log AF_b - \log AF_t)$  by  $AS_t (P_t^2 - P_b^2) / 2$  and  $AF_t (P_t^2 - P_b^2) / 2$ , respectively.

The optical thickness of line absorption is obtained, using a fit to calculations with a Malkmus model for very narrow spectral intervals and weighted by the response function of AVHRR. Using the line strengths given by Rothman *et al.* (1983), we get

$$\tau = U \times \frac{0.000067 + 0.0065 U}{1 + 115 U + 1.3 U^{1.6}}$$

The coefficients multiplying U in the numerator and denominator have been changed (previously 0.0081 and 109, respectively) to correct a small error in the model fit. Line absorption is generally much weaker than the continuum absorption.

Figure 3.11 shows the variation of these two optical thicknesses with the amount of water in a 200 mb layer at 282 K, expressed in precipitable centimeters.

Clouds are assumed to be single, physically thin layers with no vertical temperature gradients. In the cloud top temperature retrieval, all clouds are treated as opaque blackbodies (emissivity = 1) and scattering is neglected. In the adjustment step, two microphysical models are used in Mie scattering calculations to relate the visible optical thickness to the IR absorption and scattering optical thicknesses. The first model assumes a gamma distribution of water spheres with effective radius = 10  $\mu\text{m}$  and effective variance = 0.15 and uses the optical constants for liquid water from Downing and Williams (1975) for infrared wavelengths. The IR absorption optical thickness used to adjust cloud top temperatures for liquid water clouds is given by 0.39 TAU, where TAU is the visible optical thickness. The second model

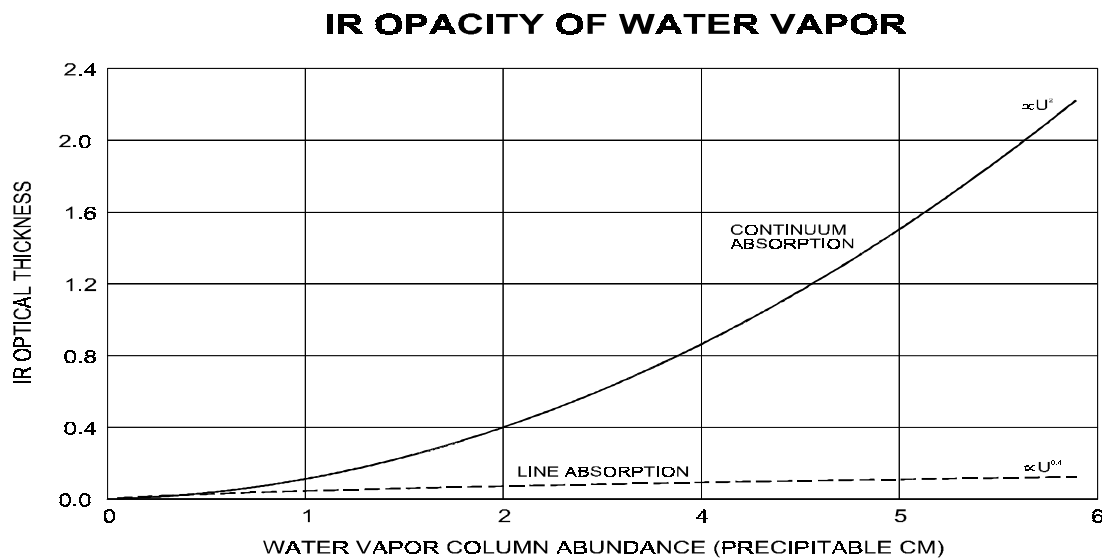


**Figure 3.11.** Variation of water vapor infrared opacity at 10.5  $\mu\text{m}$  with total water amount.

assumes a -2 power law of ice spheres between 20 and 50  $\mu\text{m}$  (effective radius = 30  $\mu\text{m}$  and effective variance = 0.10) and uses optical constants for ice from Warren (1984). The IR absorption optical thickness for ice clouds is given by 0.47 TAU (cf. Minnis et al. 1993). The scattering calculations produce two look-up tables used in the cloud analysis, one for water spheres and one for ice spheres (IR scattering is insensitive to particle shape) that give the physical cloud top temperatures as a function of the IR brightness temperature retrieved neglecting scattering, the optical thickness, and the viewing angle.

In preparation for the radiative analysis, the IR model is used to convert the TOVS atmospheric profiles of physical temperature and humidity into profiles of top-of-atmosphere brightness temperature at three satellite zenith angles ( $\mu = 0.3, 0.6, 1.0$ ) as a function of location and time by placing an opaque (emissivity = 1) surface at each pressure level. Note that the effective wavelength of the AVHRR radiometer channel is about 0.5  $\mu\text{m}$  shorter than that of the geostationary satellite radiometers, but this difference is ignored in the analysis because the geostationary radiometer calibrations are normalized to that of the AVHRR. The cloud radiative processing uses these results as a dataset for the cloud top temperature retrieval, where all clouds are treated as blackbodies (scattering neglected). The water vapor values provided in the TOVS data set are rather noisy (quoted estimates of error are about 25-35%, Smith *et al.* 1979). To reduce this noise somewhat, all water vapor values are averaged over a 5-day period centered on the day being analyzed. Also calculated are the top-of-atmosphere brightness temperature corresponding to the TOVS physical surface temperature, the total atmospheric transmission (TRANS), and the total atmospheric emission (EMISS). These quantities are calculated at nine satellite zenith angles ( $\mu = 0.2, 0.3, 0.4, \dots, 0.9, 1.0$ ).

### VIS Model

The visible radiance model is very similar to that described in Rossow *et al.* (1989), with optical constants adjusted to the spectral response of Channel 1 on the NOAA-9 AVHRR (see Rossow *et al.* 1992); however, none of the calculations are very sensitive to the precise spectral dependence or wavelength used over the range from 0.55 to 0.7  $\mu\text{m}$  covered by the satellite radiometers (the exception is the surface reflectance for vegetated land surfaces). The model represents the clear atmosphere as three gas layers above a reflecting surface; no aerosol effects are included. Each pixel is assumed to correspond to a column of gas with horizontally uniform properties; the surface and any cloud layers are also assumed to be horizontally uniform over the image pixels (4-7 km).

The three gas layers are an absorbing layer at the top, representing ozone, and two Rayleigh scattering layers (total gas amount represented by a maximum surface pressure of 1000 mb), one above and one below any cloud layer. The small effect of variations in surface pressure is ignored. Ozone absorption is calculated, using a fit to line-by-line calculations weighted by the spectral response of the AVHRR:

$$\tau = U [ 0.085 - (0.00052 U) ]$$

where U is the column amount of ozone in cm-STP. Continuum absorption strengths in the Chappuis band are from Inn and Tanaka (1953). The transmission is given by

$$\text{Tr} = \exp \{ - U [ 0.085 - 0.00052 U ] / \mu \}$$

where  $\mu$  can be the cosine of either solar or satellite zenith angle.

To calculate the effects of Rayleigh scattering, the VIS model is used to pre-calculate a look-up table of isotropic surface reflectance as a function of VIS radiance values (normalized to the mean solar constant of the instrument) and viewing/illumination geometry. Given a VIS radiance, corrected for varying sun-Earth distance and ozone absorption, and the geometry, the table provides a corresponding value of isotropic surface reflectance.

The effects of the atmosphere on the broader "visible" channel on METEOSAT satellites are slightly overestimated by the analysis. In general this difference in spectral response is insignificant, except for the retrieved surface reflectances for vegetated land areas, which will be significantly larger in areas observed by METEOSAT satellites. The difference is land surface reflectances obtained from METEOSAT is removed in Stage D2 data.

Land and sea ice covered surfaces are assumed to be isotropic reflectors. Reflection from water is specified by a model obtained by removing the atmospheric effects from the clear radiance model of Minnis and Harrison (1984). The consistency of this model has been checked by comparing it to directly retrieved surface reflectances for a summer and winter month from both polar and geostationary satellites, using the VIS retrieval model. The retrieval agrees with the model to within 2% (random error) except near glint conditions. In glint geometry the model is found to be too bright by  $\approx 5\%$  in a majority of cases, but too dark in many other cases. The model in glint geometry is based on a four month survey of observed clear sky radiances.

Clouds are assumed to be single, physically thin layers that are pure (conservative) scatterers of VIS radiation. No gaseous absorption or scattering is included in the layer. When clouds are present, the VIS radiances are calculated from the individual scattering and absorption layers using the doubling-adding procedure (Hansen and Travis, 1974); the amount of gas above the cloud is determined by the cloud top pressure and the remaining gas is below the cloud.

Visible reflectance from clouds is calculated in complete multiple scattering calculations using two cloud particle size-shape models. The first model is for liquid water clouds (cloud top temperature  $\geq 260$  K): the optical constants of liquid water are from Hale and Querry (1973) for solar wavelengths. A gamma distribution of spheres defines an effective radius of  $10 \mu\text{m}$  and a variance of 0.15 (see Hansen and Travis 1974). The second model is for ice crystal clouds (cloud temperature  $< 260$  K): the optical constants of ice are from Warren (1984). A -2 power law of ice polycrystals between 20 and  $50 \mu\text{m}$  gives an effective radius =  $30 \mu\text{m}$  and an effective variance = 0.10; the fractal scattering phase function is from Macke (1994). Figure 3.12 compares the two scattering phase functions (Mishchenko et al. 1996). In preparation for the cloud analysis, the scattering calculations are used to pre-calculate two look-up tables. The main one gives cloud optical thickness values for liquid spheres as a function of the observed VIS radiance, surface reflectance, cloud top pressure and illumination and viewing geometry. The second table matches the solutions for liquid water spheres with those for the ice polycrystals to convert liquid water optical thicknesses to ice values as a function of illumination and viewing geometry (this technique was designed by P. Minnis, NASA Langley Research Center).

Figure 3.13 shows the model relationships between TAU and the cloud spherical albedo (over a black surface) and IR (narrowband) emissivity.

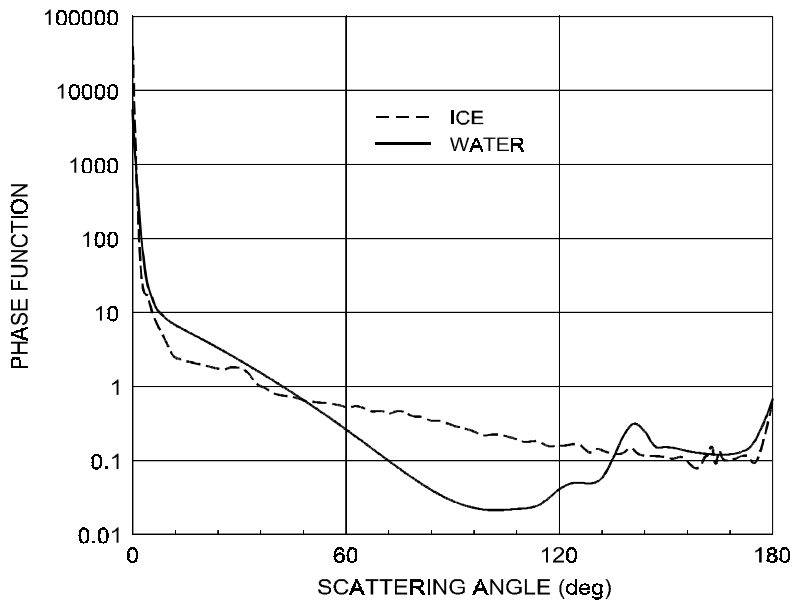


**Figure 3.12.** Scattering phase functions for 10  $\mu\text{m}$  spheres (solid curve) and 30  $\mu\text{m}$  fractal polycrystals (dashed curve) at visible wavelength (0.6  $\mu\text{m}$ ).

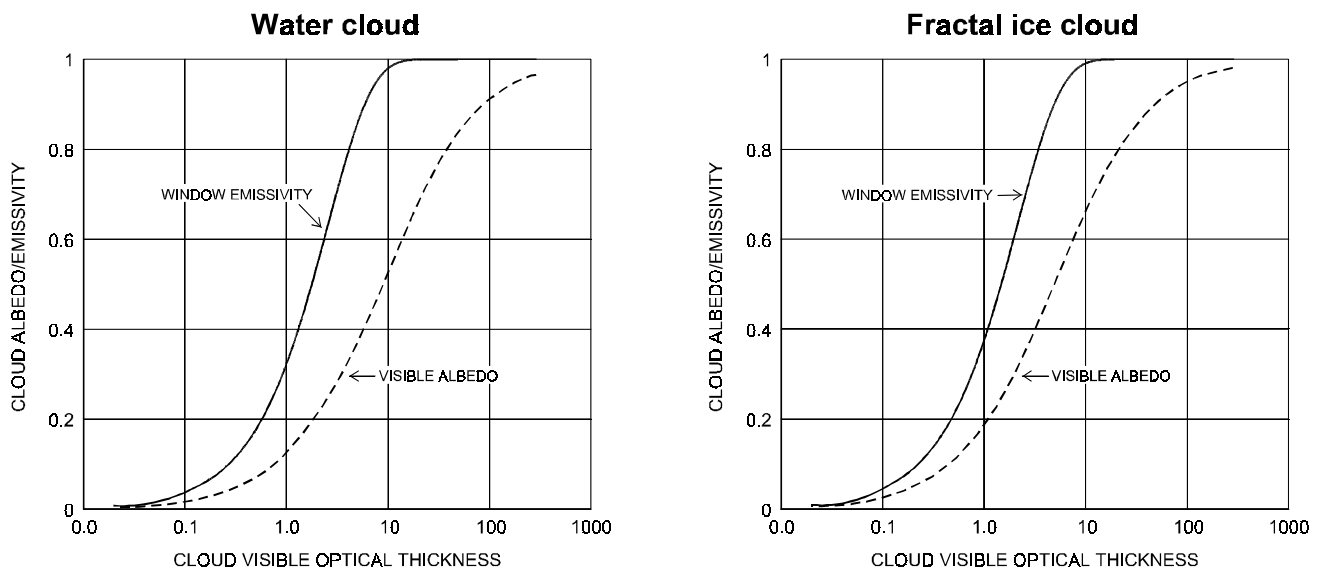


**Figure 3.13.** Relations of cloud visible (0.6  $\mu\text{m}$ ) albedo (scene albedo over black surface with no atmosphere) and infrared (10.5  $\mu\text{m}$ ) emissivity as a function of optical depth at 0.6  $\mu\text{m}$  for the liquid (left) and ice (right) water cloud models used in the ISCCP radiative analysis.

## NIR Model

In the polar regions, NIR ( $\approx 3.7 \mu\text{m}$ ) radiances are used to augment detection of clouds over snow and ice surfaces, where the VIS-based detections over such reflective surfaces are uncertain and where there appear to be numerous low-lying clouds exhibiting little temperature contrast with the surface. The threshold tests in daytime are performed on NIR solar reflectances (RNIR) after removal of the thermal emission contribution. The thermal emission at  $3.7 \mu\text{m}$  is calculated assuming a blackbody wavelength spectrum at the temperature observed at  $11 \mu\text{m}$ .

In the radiative analysis, NIR reflectances are used to aid the retrieval of cloud optical thicknesses over snow and ice surfaces. Since the reflection from snow and ice surface is more nearly isotropic than the reflection from a cloud, there are geometries at which optically thinner clouds over a snow or ice surface can appear less reflective than clear conditions. In these circumstances there are two possible cloud optical thicknesses that produce the same scene reflectance (Figure 3.14). In the C-series of the cloud retrievals, the larger optical thickness solution was always selected. Because water and ice absorb strongly at  $3.7 \mu\text{m}$ , RNIR is a strong function of particle size. Since surface ice tends to have much larger particle sizes than clouds, snow and ice surfaces are much less reflective than clouds. Thus, at  $3.7 \mu\text{m}$  the scene reflectivity increases more nearly monotonically with increasing cloud optical thickness (Figure 3.14). In the D-series of the cloud retrievals over snow and ice surfaces in the polar regions, if  $\text{RNIR} < 0.07$ , the smaller solution for visible optical thickness is used; if  $\text{RNIR} \geq 0.07$ , the larger solution is selected.

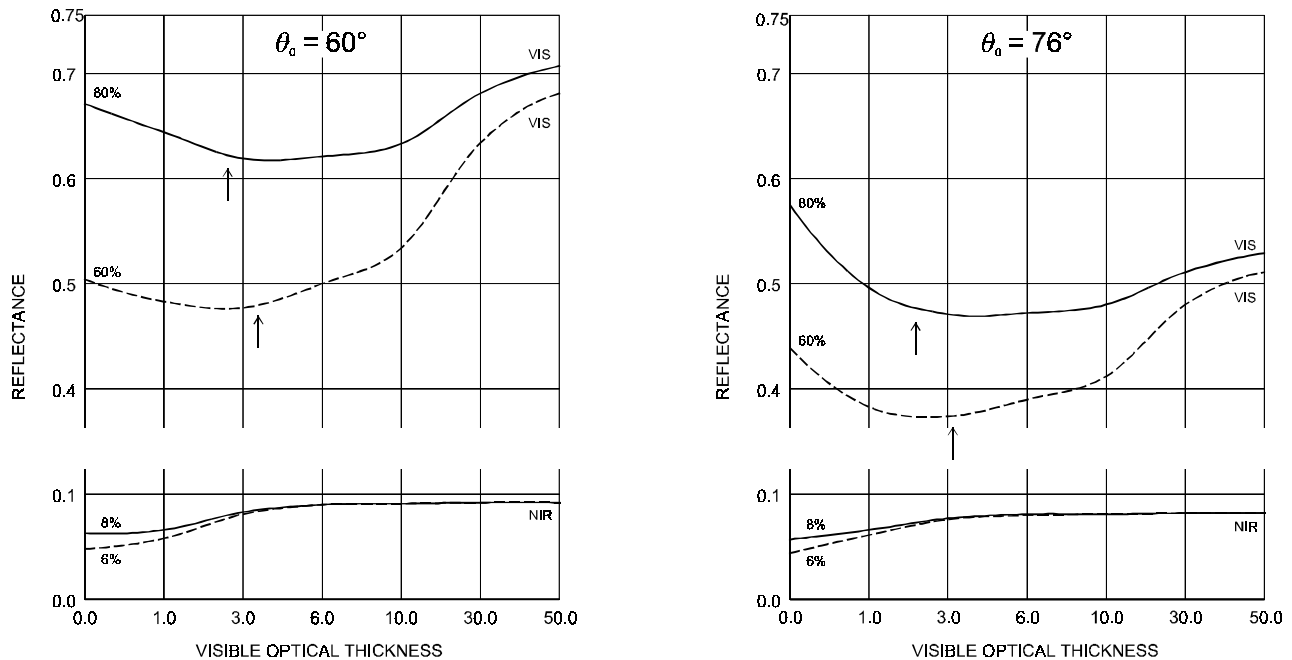


**Figure 3.14.** Variations of scene reflectances at VIS ( $0.6 \mu\text{m}$ ) and NIR ( $3.7 \mu\text{m}$ ) wavelengths as a function of cloud visible optical thickness at two solar zenith angles, 0, and two visible surface albedos, 80% (solid) and 60% (dashed). The corresponding surface albedos at  $3.7 \mu\text{m}$  are approximately equal to 8% and 6%. Arrows indicate threshold NIR reflectance and corresponding visible optical thicknesses separating the upper and lower branches of the curves.

### 3.2.5.2. CLEAR RETRIEVALS

Clear radiances from the clear sky composites are available for every pixel, whether clear or cloudy. Retrievals of surface temperature (TS) from the IR radiance and surface visible reflectance (RS) from the VIS radiance (daytime only) are performed first, so that these quantities are available for use in retrievals of cloud properties from cloudy pixels. For clear pixels, another set of values of surface temperature and visible reflectance is retrieved from the observed radiances. In both cases (composite or observed) the procedure is the same.

#### Surface Skin Temperature

The surface temperature, TS, corresponding to the clear IR radiance (brightness temperature, TOBS) is given by

$$BTS = [ BTOBS - EMISS ] / TRANS$$

where BTS is the Planck radiation of a black body (weighted by the response function of the NOAA-9 AVHRR) for the surface temperature, BTOBS is the clear IR radiance, and EMISS and TRANS are the total atmospheric emission and transmission calculated with the IR radiance model from the TOVS atmospheric data and interpolated to the value of  $\mu$  for the particular observation. TS is obtained from BTS by inverting the Planck function (weighted by the AVHRR response). Since the atmosphere is relatively transparent at 11  $\mu\text{m}$  wavelength, TS corresponds to the **brightness** temperature of the surface skin; the physical temperature of surfaces with 11  $\mu\text{m}$  emissivities  $< 1$  will be larger. The corresponding pressure is the surface pressure from TOVS.

Although this formula is theoretically correct, when the water opacity becomes very large, TRANS becomes very small. Then errors in the observed radiances, in the inference of the clear IR radiance and in the properties of the atmosphere are multiplied by a very large number,  $(1/TRANS)$ . This is equivalent to saying that, when TRANS is small, the measured signal contains little actual information about the surface and is dominated by the atmospheric emission. This "de-coupling" of the observations from the surface properties is also indicated by large differences between the surface emission and the top-of-atmosphere emission. Such conditions occur in the tropics when satellite zenith angles are relatively large. Thus, whenever  $TRANS < 0.25$  or the calculated surface and top-of-atmosphere emission difference exceeds a threshold, an alternate procedure is used to estimate surface temperature:

$$BTS = BTOBS + [ BTST - BTBT ]$$

where BTST is the Planck radiation corresponding to the TOVS surface temperature and BTBT is the corresponding top-of-atmosphere brightness temperature calculated for the TOVS temperature/humidity profile at the same viewing geometry. In other words, we assume, in cases of large water vapor opacity, that the difference between the observed brightness temperature and the actual surface temperature is the same as it is for the TOVS values. This is approximately equivalent to assuming that the atmospheric and surface temperatures vary together, i.e., that if the actual surface temperature is higher than the TOVS value, so is the atmospheric temperature which dominates the observed radiances. This assumption appears accurate over tropical oceans but less accurate over tropical land areas, especially deserts.

### Surface Visible Reflectance

The VIS radiances are corrected to a constant sun-Earth distance. Ozone absorption is removed by dividing by the two transmission factors (for the solar-to-surface and surface-to-satellite pathlengths). The corrected clear VIS radiances are then compared to the pre-calculated look-up table which gives isotropic surface reflectances as a function of  $\mu = \cosine$  satellite zenith angle,  $\mu_0 = \cosine$  solar zenith angle, and  $\phi = \text{relative azimuth angle}$ .

### **3.2.5.3. CLOUD RETRIEVALS**

For each cloudy pixel, cloud top temperature (TC), cloud top pressure (PC) and cloud optical thickness (TAU) are retrieved.

#### Cloud Top Temperature - Pressure (opaque limit)

The first retrieval of the cloud top temperature assumes that the cloud is opaque to IR radiation (emissivity = 1) and uses the pre-calculated profiles of IR brightness temperatures at three satellite zenith angles ( $\mu = 0.3, 0.6, 1.0$ ) corresponding to the physical atmospheric temperatures at various pressure levels for the particular location and time. These values are interpolated to the particular satellite zenith angle of the pixel, using

$$T(\mu) = C (1/\mu - \mu) [ T_L - T_U ] + R_L T_U - R_U T_L$$

where either  $0.3 \leq \mu < 0.6$  or  $0.6 \leq \mu \leq 1.0$ ,  $T_L$  and  $R_L = C * (1/\mu - \mu)$  are the brightness temperature and the coefficient at the lower value of  $\mu$ , and  $T_U$  and  $R_U = C * (1/\mu - \mu)$  are the values at the higher value of  $\mu$  in either interval. The value of  $C$  in the two intervals is calculated from

$$C^{-1} = (1/\mu - \mu)_L - (1/\mu - \mu)_U$$

The brightness temperature of the cloudy pixel is compared to the values interpolated to the satellite zenith angle of each pixel to find a match at some pressure level (which can be interpolated between the values on the profile); the corresponding physical temperature and pressure are then reported as the cloud top temperature and pressure. If the observed cloudy brightness temperature is less than any value on the TOVS profile, then the cloud top temperature is set equal to the brightness temperature (since the opacity of the water vapor above the tropopause is negligible) and the cloud top pressure is calculated using the hydrostatic equation above the tropopause level. If the observed brightness temperature is warmer than any value on the TOVS profile (the surface air temperature is the warmest value and is obtained by extrapolating the atmospheric temperature profile to the surface, but this may not correspond to the surface skin temperature inferred from the satellite-measurements), then the cloud top pressure is set equal to the surface pressure and the cloud top temperature is retrieved using the surface temperature procedure described above. If an isothermal or inversion layer exists in the atmospheric temperature profile, the uppermost point with the same temperature is used to determine cloud top pressure.

## Visible Optical Thickness

Cloud optical thicknesses are retrieved by comparing observed VIS radiances with values pre-calculated from the radiative model. These values are in a table that relates the liquid water cloud visible optical thickness, TAUW, to the VIS radiance (corrected for sun-Earth distance and ozone absorption), the viewing/illumination geometry, the surface reflectance from the clear sky composite value of the VIS radiance, and the cloud top pressure from the IR radiance analysis. Interpolation errors in this table are less than 10%, relative; interpolation errors are reduced in the D-series analysis, especially at low optical thicknesses, by changing to an interpolation that is linear in the logarithm of optical thickness. This change also eliminated the occasional occurrence of negative optical thickness values at low VIS radiances. A value of TAUW is obtained for all cloudy pixels.

At some illumination/viewing geometries over highly reflective surfaces, there are two possible values of TAUW that give the same VIS radiance. Because cloud reflectances are more anisotropic than most surface reflectances, there are situations where adding cloud (usually with relatively low optical thicknesses) to a scene can decrease the reflectance. This situation occurs much more frequently for surface reflectances  $> 0.5$ . In the C-series cloud analysis, the larger of the two values of TAUW was always selected. In the D-series analysis, whenever AVHRR data are analyzed over snow and ice-covered surfaces, the part of the  $3.7 \mu\text{m}$  radiances that is reflected sunlight (RNIR) is used to select either the smaller or larger value of TAUW: if  $\text{RNIR} \leq 0.07$ , the smaller value of TAUW is used.

In the D-series cloud analysis, ice cloud visible optical thickness values, TAUI, are also retrieved for each cloudy pixel. The values of TAUI are obtained from a pre-calculated table that matches values of TAUW and TAUI that produce the same VIS radiances for the same illumination/viewing geometry (a procedure developed by P. Minnis at NASA Langley Research Center -- cf. Minnis et al. 1993). However, for very large VIS radiances and certain illumination/viewing geometries there are situations for which there is no value of TAUI corresponding to TAUW because the asymptotic reflectivity for the larger ice crystals is lower than for the smaller liquid water spheres. In such cases, a second table that matches optical thicknesses giving the same visible **albedo** is used to estimate values of TAUI. Values of TAUI are reported for all cloudy pixels with ice cloud top temperature is  $< 273 \text{ K}$ .

## Cloud Top Temperature Adjustments

The value of the cloud optical thickness is checked for consistency with the assumption that the clouds are opaque to IR radiation. The optical thickness value calculated in the VIS model (TAU-VIS) is the value at  $0.6 \mu\text{m}$  wavelength. In the C-series of the analysis an empirical value (2.00) of the ratio TAU-VIS/TAU-IR was used to get TAU-IR. In the D-series a Mie scattering radiation code is used to calculate the optical thickness at  $10.7 \mu\text{m}$  wavelength (TAU-IR) for both TAUW ( $10 \mu\text{m}$  particle radius) and TAUI ( $30 \mu\text{m}$  particle radius). Use of spherical shapes for calculating this ratio is acceptable because the infrared scattering is insensitive to particle shape (cf. Minnis et al. 1993). The ratios obtained are  $\text{TAUW-VIS/TAUW-IR} = 2.56$  and  $\text{TAUI-VIS/TAUI-IR} = 2.13$ .

The observed IR radiance is modeled as the sum of two contributions: the emission from the cloud layer and the transmitted radiation from the surface (the results are corrected for weak scattering effects in a subsequent step). To account for water vapor absorption below the cloud, which is the majority of the

total, we use the clear sky radiance at top-of-atmosphere to represent the radiation coming from the surface and the lower atmosphere:

$$\text{BTOBS} = (1 - \text{TRANS}) \times \text{BTC} + \text{TRANS} \times \text{BTS}$$

where BTOBS is the observed radiance (Planck function for a temperature, TOBS, weighted by the spectral response function of NOAA-9), BTC is the radiance emitted by a cloud with temperature, TC, and emissivity (1 - TRANS), and BTS is the clear sky (surface) brightness temperature. The transmission of the cloud is given by

$$\text{TRANS} = \exp [ - \text{TAU-IR} / \mu ]$$

where  $\text{TAU-IR} = \text{TAUW}/2.56$  or  $\text{TAUI}/2.13$ .

If  $\text{TAU-IR}/\mu > 5.5$ , the cloud is considered opaque (since  $\text{TRANS} < 0.5\%$ ) and no adjustment of TC is required. If  $\text{TAU-IR}/\mu \leq 5.5$ , then an adjusted cloud top temperature is obtained from:

$$\text{BTC} = [ \text{BTOBS} - \text{TRANS} \times \text{BTS} ] / (1 - \text{TRANS})$$

The adjusted cloud top pressure that corresponds to TC is found from the temperature profile. If TC is smaller than any value on the profile, the cloud top pressure is calculated as a value smaller than the tropopause value using the hydrostatic formula.

This procedure encounters difficulties with very thin clouds because of errors in the VIS radiance measurements, uncertainties in the determination of the retrieved surface reflectances and temperatures, and in the retrieval of TAU-VIS and TAU-IR. In other words, even though a cloud may be "obvious" in the IR image, its VIS radiance effect may be negligible (dust storms also produce this effect), making an accurate determination of its optical thickness (which is near zero) difficult. This can lead to non-physical relations in the above equation for BTC. Also when (1 - TRANS) is too small, all of these errors are amplified.

Thus, we also solve the equation for a minimum value of TAU-IR (TAU-MIN) by assuming TC to be 5 K colder than the tropopause temperature:

$$\text{TRANS-MAX} = [ \text{BTOBS} - \text{BTC-MIN} ] / [ \text{BTS} - \text{BTC-MIN} ]$$

where TAU-MIN is obtained from  $\text{TRANS-MAX} = \exp [ - \text{TAU-MIN} / \mu ]$ . If  $\text{TRANS-MAX} \geq 1$  (ie, the observed brightness temperature is greater than or equal to the clear sky brightness temperature as might occur for a dust storm cloud), no correction of TC is performed. If  $\text{TRANS-MAX} < 0.001$  (ie, the observed brightness temperature is colder than the minimum temperature as can occur over high topography, especially in the polar regions), no correction of TC is performed as this cloud already appears to be in the lower stratosphere. If the optical thickness retrieved from VIS radiances is less than this minimum value or if the transmitted radiance calculated from the retrieved optical thickness exceeds the observed IR radiance, then the cloud top temperature is set to the tropopause temperature minus 5 K (cloud pressure equals tropopause pressure) and the optical thickness is set to its minimum value.

If the values of the cloud top temperature and pressure are adjusted and the value of TAU has not been re-set to the minimum value, then the retrieval of TAU-VIS is repeated with the new cloud top pressure. The cycle of retrievals is repeated until the values converge (usually no more than one iteration is needed but if more than ten iterations are performed the pixel is discarded). Adjustment of the values of cloud top temperature and pressure is performed only during the daytime.

### IR Scattering Adjustment

During daytime there is an additional small adjustment of cloud top temperatures and pressures for the viewing angle-dependent effects of scattering at IR wavelengths. The scattering correction is calculated from the Mie scattering radiation code for water and ice spheres, since the particle shape has little effect on the results. The scattering effect causes a small increase of brightness temperatures when a cloud is viewed from the near-nadir direction as compared with other directions. If the adjusted cloud top temperature differs from the original value by  $\leq 0.3$  K, no adjustment is made. If the retrieved cloud top temperature is more than 5 K larger than the clear sky IR radiance, no adjustment is performed.